Research paper   **Open Access**

Investigation of caffeic acid as an inhibitor for aluminum-silicon alloy corrosion

Mona A. El-Etre
Department of Basic Science, Faculty of Engineering, Benha University, Benha, Egypt
e-mail: monaeletr@yahoo.com

Abstract

Caffeic acid was investigated as an inhibitor for aluminum-silicon alloy corrosion in 1.0 M solution of hydrochloric acid. Weight loss, Tafel polarization, and impedance spectroscopy techniques were used in the study. The data showed that caffeic acid act as an excellent inhibitor for acid corrosion of the aluminum alloy. The inhibition efficiency was found to be increased with its concentration but decreases with increasing temperature. The inhibition process was attributed to adsorption of the inhibitor molecules on the alloy surface. The adsorption is physical in nature and follows Langmuir adsorption isotherm. Thermodynamic functions of the corrosion reaction were determined and discussed.

Keywords: Aluminum-silicon alloy, acid corrosion, natural corrosion inhibitor.

Received; 20 July 2019, Revised form; 22 Aug. 2019, Accepted; 22 Aug. 2019, Available online 1 Oct. 2019.

1. Introduction

Aluminum alloys are widely used in different industrial application. Among these, aluminum-silicon alloys are characterized by some improved properties such as hardness, casting, and welding. They are usually used in the manufacturing of heat exchangers. As aluminum is the main component of the alloys, they use the same root for withstanding corrosion by formation of an isolating oxide film at their surfaces. However, in many cases using corrosion inhibitors is necessary, especially when they are exposed to highly aggressive media.

Caffeic acid (3,4-dihydroxycinnamic acid) is a phenolic acid could be found in a large number of plants like tomato, strawberry, and carrot [1-3]. Literature survey showed that many pieces of research were conducted for investigation of phenolic acids as corrosion inhibitors for different alloys [4-12]. It was reported that plant extracts containing caffeic acids derivatives showed good corrosion inhibition efficiency [13, 14]. On the other hand, there are only a few reports on the corrosion inhibition performance of caffeic acid in the literature. Caffeic acid was found to be good corrosion inhibitor for iron and aluminum [14], copper [11, 14] as well as for aluminum-silicon alloy in sulfuric acid [15].
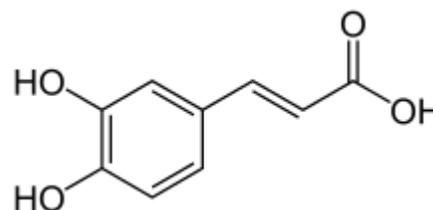

Fig (1): Caffeic acid

2. Experimental

The chemical composition of aluminum-silicon alloy used in this study is presented in table (1). Specimens with the dimension of 1.6 x 1.5 x 0.7 cm were used in the weight loss measurements. Prior to each experiment, the surface of every specimen was mechanically polished with different grades of emery papers, cleaned with acetone and distilled water then dried at room temperature before use.

Table (1): Chemical composition of the aluminum-silicon alloy (6063).

Si	Fe	Cu	Mn	Mg	Ni	Ti	Zn	Na	Al
0.42	0.17	0.001	0.009	0.42	0.001	0.010	0.001	0.0012	

The used aggressive medium is 1.0 M HCl solution. The concentration of the acid was adjusted by titration against a standard solution of sodium carbonate. A stock solution of caffeic acid was prepared by dissolving an exact weight in distilled water. The used concentrations of it were prepared by dilution.

Every experiment has been conducted three times and the average weight loss of them was recorded. The inhibition efficiency (η) and the fraction of surface covered by the additive (θ) were calculated using the following equations, respectively:

$$\eta = \left(\frac{W_f - W_i}{W_f} \right) x\ 100$$

$$\theta = \left(\frac{W_f - W_i}{W_f} \right)$$

where W_f and W_i are weight loss in free and inhibited solutions, respectively.

A three-electrode cell with platinum as a counter electrode and saturated calomel electrode (SCE) as a reference electrode, was used for the electrochemical measurements. Aluminum-silicon alloy working electrode is a rode impeded in a glass tube with Araldite leaving an exposed bottom side with an area of 0.48 cm² contacted to the corrosive solution. The exposed surface was abraded with different grades of emery papers, rinsed with distilled water and acetone then dried between two filter papers, before inserting in the test solution. The electrode was lifted in the test solution until it reaches a steady-state potential value before starting the measurements. Corrosion parameters, as well as impedance parameters, were obtained using Metrohm potentiostat supported with Nova software for calculations. The potentiodynamic polarization measurements were obtained using a scan rate of 2 mVs⁻¹ at 25 ± 1 °C or other mentioned temperatures. The inhibition efficiency (η) obtained from electrochemical polarization and impedance spectroscopy were calculated using the following equations, respectively:

$$\eta = \left(\frac{I_f - I_i}{I_f}\right) x\ 100$$

$$\eta = \left(\frac{R_{ct,i} - R_{ct,f}}{R_{ct,i}}\right) x\ 100$$

where, I_f and I_i, are corrosion current density for the free and inhibited solutions. On the other hand, $R_{ct,f}$, and $R_{ct,\ I}$ are the charge transfer resistance for the free and inhibited solutions respectively.

3. Results and discussion
3.1. Corrosion rate measurements
3.1.1. Weight-loss technique

Table (2) contains the inhibition efficiency values as a function of inhibitor concentration and the exposure time of the alloy to the corrosive medium. Inspection of the table reveals that; the inhibition efficiency increases as the inhibitor concentration is increased as well as increasing exposure time. Fig (2) presents the relation between inhibitor concentration and inhibition efficiency at different exposure times. It could be seen from the figure that the inhibition efficiency increases sharply in a narrow range of increasing concentration. Nevertheless, as the concentration reaches a certain value, the inhibition efficiency steeply increases with further inhibitor concentration increment.

Table (2): Inhibition efficiency as a function of inhibitor concentration and the exposure time.

Conc., M t, h	$5x10^{-6}$	$1\ x10^{-5}$	$5\ x10^{-5}$	$1\ x10^{-4}$	$5\ x10^{-4}$
1	80.29	89.78	95.62	97.08	99.27
2	85.02	94.66	95.97	97.57	99.72
3	89.03	95.55	96.36	97.63	99.75
4	91.83	95.7	96.6	97.72	99.78

These findings suggest that the inhibition process takes place through adsorption of the inhibitor molecules at the electrode surface. The adsorbed molecules form an isolating layer prevents the reach of the aggressive solution to the electrode surface. As the number of the molecules increases the film become more compact and thus increasing the inhibition efficiency. In the same manner, the number of adsorbed molecules increases with time leading to the same effect.
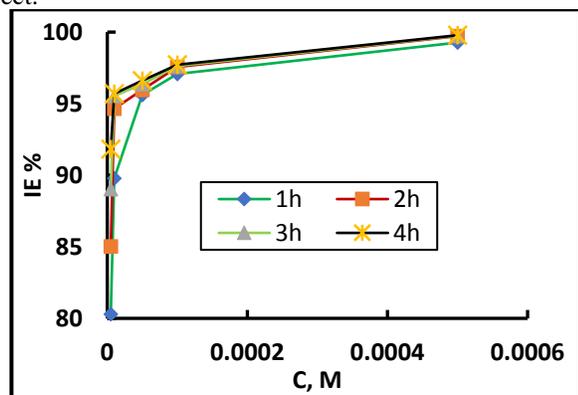

Fig (2): Relation between inhibitor concentration and

On the other hand, the inhibitor achieves its high impact at a very small concentration range, after it the effect of increasing concentration is markedly diminished. This result suggests that only a small number of the inhibitor molecules are enough to cover most of the alloy surface leading to high inhibition efficiency. Behavior like this could be explained by the horizontal adsorption of the inhibitor molecules at the alloy surface. Recalling the inhibitor molecule structure, one can conclude that the molecule is attracted to the alloy surface through the oxygen atoms present at both ends. This mode of adsorption forces the aromatic ring to be adsorbed horizontally on the surface covering the highest possible area.

3.1.2. Polarization technique

The corrosion rates of aluminum alloy in 2 M HCl free and inhibited solutions were determined by Tafel polarization method. Cathodic and anodic polarization curves are represented in fig. 3. It could be seen that the curves are shifted toward less current in the presence of the increasing concentrations of the inhibitor. This behavior confirms the inhibition effect of the added compound.

Table 3 contains the values of corrosion potential, Tafel constants, corrosion current density and the inhibition efficiency obtained from polarization technique. The table shows that the corrosion potential and both Tafel constants change slightly suggesting that caffeic acid acts as a mixed corrosion inhibitor. According to this inhibition mechanism, the caffeic acid molecules adsorb on both anodic and cathodic sites at the alloy surface.
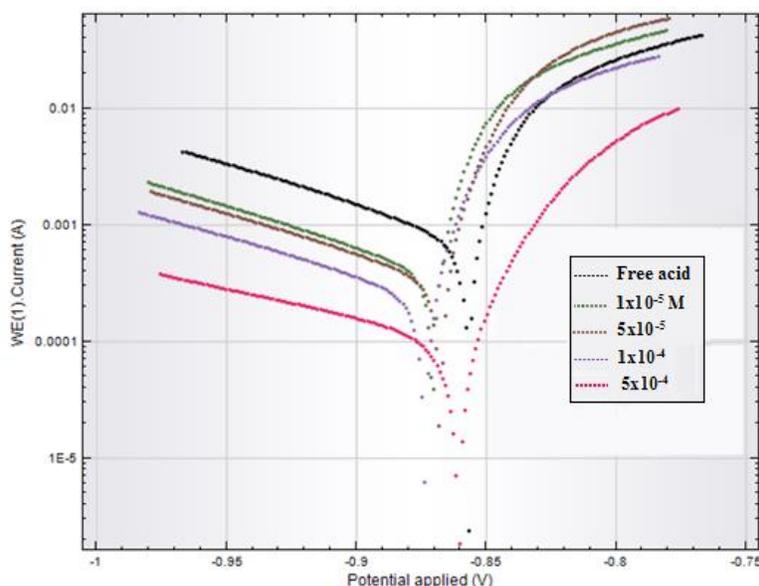
Fig (3): polarization curves for aluminum-silicon alloy in free and inhibited 2 M HCl solutions.

Table (3): Corrosion parameters as revealed from Tafel polarization technique.

Conc., $Mx10^5$	$-E_{corr}$, mV	β_a mV/decade	β_c mV/decade	I_{corr} mA/cm2	IE%
Free	925	134	120	2.3	----
1	969	137	135	2.0	12.16
5	966	142	116	1.6	27.98
10	953	142	107	0.85	62.57
50	890	195	97	0.14	93.85

3.1.3. Impedance spectroscopy technique

The aluminum-silicon alloy corrosion rates 2 M HCl free and inhibited solutions were studied using impedance spectroscopy technique. Fig. (4) shows the Nyquist diagram obtained for the alloy in free and increasing concentrations of caffeic acid. Almost perfect semicircles were obtained. The radius of the semicircle increases with increasing the additive concentration. Fig (5) represents the Randles equivalent circuit which fit with the obtained Nyquist diagram. The Randles equivalent circuit is one of the simplest possible models describing processes at the electrochemical interface [16]. It consists of an electrolyte resistance R_S in series with the parallel combination of the double-layer capacitance C_{dl} and charge transfer resistance Rct.

Table (4) contains the impedance parameters drawn from the Nyquist diagram. The data of the table show that the charge transfer resistant increases in the presence of the increasing concentration of the inhibitor. This result suggests the formation of an isolating layer of the adsorbed molecules between the metal and the corrosive solution.
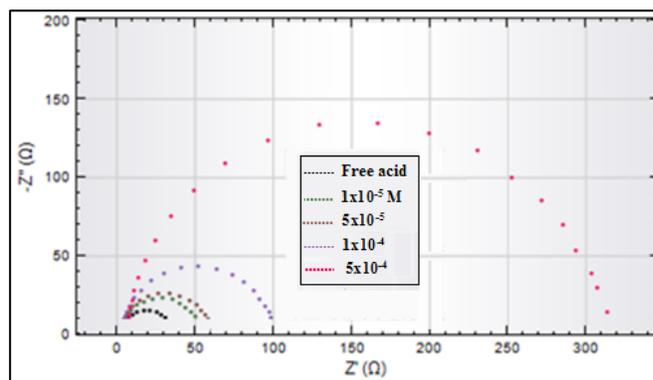

Fig (4): Nyquist diagram obtained for the alloy in free and increasing concentrations of caffeic acid.
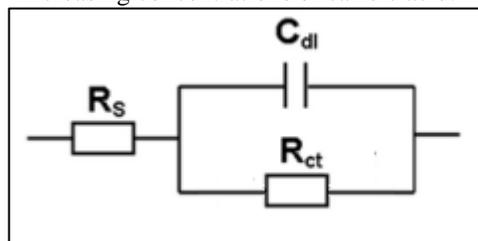

Fig (5): Rnadles equivalent circuit.

Table (4): Corrosion parameters as revealed from Impedance technique.

Conc., $M \times 10^5$	C_{dl} μF	R_S Ω	R_{ct} Ω	IE%
Free	35.21	1.74	33.44	---
1	24.19	1.77	54.96	39.15
5	21.06	2.98	61.00	45.18
10	24.53	3.93	97.75	65.79
50	23.00	5.95	305.33	89.05

3.2. Adsorption behavior

The adsorption of inhibitor molecules on the metal surface is the start step of the inhibition process. Such adsorption leads to isolating the metal surface from the corrosive medium by the adsorbed molecules film. Finding the suitable adsorption isotherm for the tested system permits a good understanding of the nature of the adsorption process. After trying many known adsorption isotherms, it was found that Langmuir adsorption isotherm is the best one consonant with the obtained experimental results.

Langmuir adsorption isotherm could be represented by the equation [17]:

$$\frac{C}{\theta} = \frac{1}{k} + C$$

Where C is the molar inhibitor concentration, θ represents the fraction of surface coverage and k is the adsorption constant which is identified as:

$$lnk = ln\frac{1}{55.5} - \frac{\Delta G^o_{ads}}{RT}$$

Where ΔG^o_{ads} is the standard adsorption free energy and the value of 55.5 is the molar concentration of water.
Fig (6) represents the relation of Langmuir adsorption isotherm. A straight line with sloop very close to one is obtained. It was found that the value of the standard free energy of adsorption ΔG^o_{ad} is - 44.92 kJ.mol^{-1}. The negative sign of the adsorption free energy indicates that the adsorption process is spontaneous. On the other hand, the high numerical value suggests a chemical adsorption process [18].
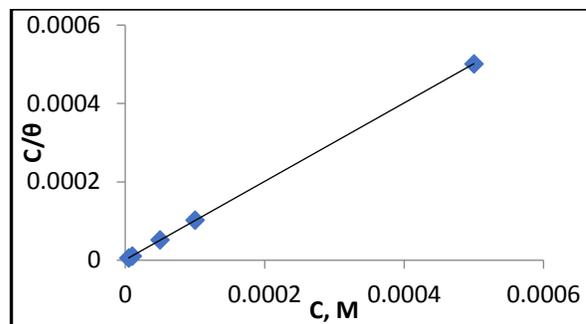

Fig (6): Langmuir adsorption isotherm

3.3. Effect of temperature

The corrosion parameters were obtained for aluminum-silicon alloy in 1.0 M HCl solutions free and containing 5 x10^{-4} M of caffeic acid at the temperature range of 30-70 °C. The results are presented in Table 3. Investigation of table 3 reveals that the corrosion rate increases as the temperature increases. On the other hand, the inhibition efficiency of the extract decreases with increasing temperature. At 70 °C the inhibition efficiency dramatically decreases and even acquires negative values with exposure times longer than one hour. This result suggests that the adsorption of inhibitor molecules on the metal surface is physical in nature. Thus, upon increasing the temperature, desorption of some adsorbed molecules takes place leading to a decrease in the inhibition efficiency. It is of interesting to note that this result seems to be discrepant with that concluded from adsorption behavior results. However, this contradiction could be understood if we take into account that the adsorption process starts physically under the effect of electrostatic charges. As the molecules reach the double layer, a chemical reaction takes place between them and the corroded metal cations. Nevertheless, the formed compound is more or less unstable and so it undergoes decomposition at high temperature. This interprets the increase of corrosion rate in the presence of inhibitor higher than in free acid, at high temperature. In this case, the presence of inhibitor molecules attracts the metal cations to the chemical reaction followed by decomposing of its products.

Table (5): Effect of temperature on corrosion rate and inhibition efficiency.

T, K \ t, h		303	313	323	333	343
Free	wt loss	0.067	0.075	0.081	0.092	0.096
1	wt loss	0.0001	0.0023	0.0051	0.0775	0.095
	IE%	99.27	97.35	97.27	63.85	1.51
2	wt loss	0.0003	0.0054	0.0183	0.196	0.374
	IE%	99.72	97.14	90.36	32.39	-3.6
3	wt loss	0.0005	0.0093	0.0452	0.2515	0.4566
	IE%	99.75	96.71	84.54	21.8	-23.04
4	wt loss	0.0006	0.0146	0.0626	0.3221	0.5322
	IE%	99.78	95.15	80.74	12.02	-39.28

The corrosion reaction can be regarded as an Arrhenius-type process which follows the equation [19]:

$$\log r = \log A - \frac{E_a}{2.303\,RT}$$

Where (r) represents the rate of corrosion reaction, A is Arrhenius factor and E_a is the apparent activation energy of the corrosion reaction. Plotting of log r (at one hour) versus 1/T gave a straight line, as shown in Fig (7). The values of activation energies for corrosion reactions of carbon steel in free and inhibited acid solutions were presented in Table (5).

Other activation parameters were calculated using the transition state equation [20]:

$$\log \frac{r_{corr}}{T} = \left[\log \left(\frac{R}{hN} \right) \right] + \left[\frac{\Delta S^*}{2.303\,R} \right] - \frac{\Delta H^*}{2.303\,RT}$$

where R is the universal gas constant (8.314 J/mol.K), N is the Avogadro's number (6.02×10^{23}), h is the Plank's constant (6.62×10^{-34} m^2 kg /s) where ΔS^* and ΔH^* are the entropy and the enthalpy changes of activation corrosion energies for the transition state complex, respectively. Plotting log (r_{corr}/T) versus 1/T gives straight lines (Fig 8) from which the activation parameters are determined and represented in Table (6). The data of table 6 show a dramatic increase in the activation energy in the presence of caffeic acid. This result supports the physical nature of inhibitor adsorption. The enthalpy of activation is positive values for both free and inhibited solutions reflecting an endothermic formation of the activated complex. While the value of entropy change in free acid is negative it turns positive in presence of the inhibitor. This result suggests that the disorder decreases going to activated complex formation in the free acid while increases in presence of inhibitor. Thus, the formation of the activated complex involves association in free acid solution and dissociation in inhibited one. The free energy values are positive for both solutions indicating instability of the activated complex.
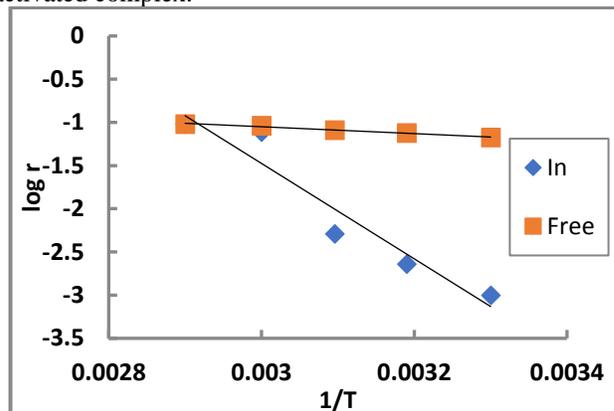

Fig (7): Arrhenius plots for corrosion of aluminum alloy in free and inhibited acid.
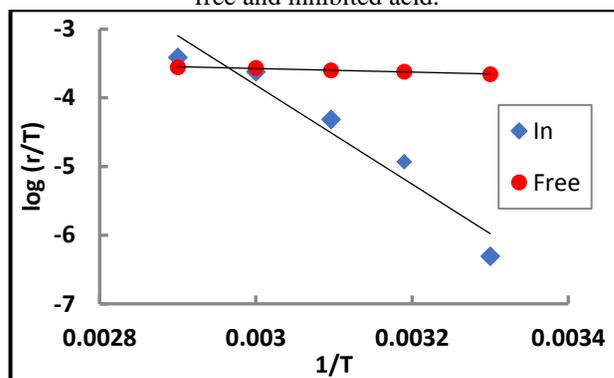

Fig (8): Transition state plots for corrosion of aluminum alloy in free and inhibited acid.

Table (6): The activation parameters of corrosion of aluminum alloy in free and inhibited acid.

	Ea, kJ.mol^{-1}	ΔH^*, kJ.mol^{-1}	ΔS^*, J.mol^{-1}K^{-1}	ΔG^*, kJ.mol^{-1} (303K)
Free	7.61	5.014	-30.18	14.16
Inhibited	105.75	138.05	17.26	132.82

4. Conclusions

- Caffeic acid act as an excellent inhibitor for acid corrosion of the aluminum alloy.
- The inhibition efficiency increases with its concentration and decreases with increasing temperature.
- The inhibition process was attributed to adsorption of the inhibitor molecules on the alloy surface.
- The adsorption is physical in nature and follows Langmuir adsorption isotherm.

References

[1] İ. Gülçin, Toxicology, 217 (2006) 213-220.

[2] J. Sochor, O. Zitka, H. Skutkova, D. Pavlik, P. Babula, B. Krska, A. Horna, V. Adam, I. Provaznik, R. Kizek, Molecules, 15 (2010) 6285-6305.

[3] T. Sun, P.W. Simon, S.A. Tanumihardjo, Journal of agricultural and food chemistry, 57 (2009) 4142-4147.

[4] L. Narvaez, E. Cano, D.M. Bastidas, Journal of applied electrochemistry, 35 (2005) 499-506.

[5] L. Vrsalović, M. Kliškić, S. Gudić, International Journal of Electrochemical Science, 4 (2009) 1568-1582.

[6] L. Vrsalović, M. Kliškić, J. Radošević, S. Gudić, Journal of applied electrochemistry, 37 (2007) 325-330.

[7] L. Vrsalović, E. Oguzie, M. Kliškić, S. Gudić, Chemical Engineering Communications, 198 (2011) 1380-1393.

[8] G.B. Mohammad Ramezanzadeh, Bahram Ramezanzadeh, Journal of Molecular Liquids

290 (2019) 111212.
[9] Y. Fang, B. Suganthan, R.P. Ramasamy, Journal of Electroanalytical Chemistry, 840 (2019) 74-83.
[10] D. Daoud, D. Ghobrini, 2018 6th International Renewable and Sustainable Energy Conference (IRSEC), IEEE, 2018, pp. 1-4.
[11] L. Vrsalović, S. Gudić, D. Gracić, I. Smoljko, I. Ivanić, M. Kliškić, E.E. Oguzie, Int. J. Electrochem. Sci, 13 (2018) 2102-2117.
[12] E. Alibakhshi, M. Ramezanzadeh, S. Haddadi, G. Bahlakeh, B. Ramezanzadeh, M. Mahdavian, Journal of cleaner production, 210 (2019) 660-672.
[13] L.C. Pirvu, Polyphenols and Herbal-Based Extracts at the Basis of New Antioxidant, Material Protecting Products, Developments in Corrosion Protection, IntechOpen, 2014.
[14] L. Vrsalović, S. Gudić, M. Kliškić, E.E. Oguzie, L. Carev, Int. J. Electrochem. Sci, 11 (2016) 459-474.
[15] F.S. de Souza, A. Spinelli, Corrosion science, 51 (2009) 642-649.
[16] J.E.B. Randles, Discussions of the faraday society, 1 (1947) 11-19.
[17] I. Langmuir, Journal of the American Chemical society, 40 (1918) 1361-1403.
[18] F. Donahu, K. Nobe, J Electrochem Soc, 112 (1965) 886-891.
[19] M.S. Silberberg, Chemistry, fourth ed., McGraw-Hill, NY, 2006.
[20] K.J.M. Laidler, John H., Physical Chemistry 1st ed., Benjamin/Cummings., 1982.